

Hyperbolic Curvature Graph Neural Network

Menglin Yang, Min Zhou, Lujia Pan, and Irwin King,

Abstract—Hyperbolic space is emerging as a promising learning space for representation learning, owing to its exponential growth volume. Compared with the flat Euclidean space, the curved hyperbolic space is far more ambient and embeddable, particularly for datasets with implicit tree-like architectures, such as hierarchies and power-law distributions. On the other hand, the structure of a real-world network is usually intricate, with some regions being tree-like, some being flat, and others being circular. Directly embedding heterogeneous structural networks into a homogeneous embedding space unavoidably brings inductive biases and distortions. Inspiringly, the discrete curvature can well describe the local structure of a node and its surroundings, which motivates us to investigate the information conveyed by the network topology explicitly in improving geometric learning. To this end, we explore the properties of the local discrete curvature of *graph topology* and the continuous global curvature of *embedding space*. Besides, a Hyperbolic Curvature-aware Graph Neural Network, HCGNN, is further proposed. In particular, HCGNN utilizes the discrete curvature to lead message passing of the surroundings and adaptively adjust the continuous curvature simultaneously. Extensive experiments on node classification and link prediction tasks show that the proposed method outperforms various competitive models by a large margin in both high and low hyperbolic graph data. Case studies further illustrate the efficacy of discrete curvature in finding local clusters and alleviating the distortion caused by hyperbolic geometry.

Index Terms—hyperbolic geometry, graph neural network, Ricci curvature

I. INTRODUCTION

Graph Neural Networks (GNNs) have garnered considerable interest recently [1], [2], [3], [4]. The majority of GNNs learn node representations in Euclidean space since it is intuition-friendly and has a number of computationally advantageous qualities [5], [6], [7]. Despite the effectiveness of Euclidean models in graph embedding, their representation ability of Euclidean space to embed complex patterns is fundamentally constrained by its polynomially expanding capacity. Although non-linear approaches assist to ameliorate this problem, complicated network patterns may still demand a computationally infeasible embedding dimensionality [8]. Moreover, the embedding quality is strongly connected to the matches between the embedding space and graph structure, as a graph may be seen as a discrete approximation to a manifold and a manifold as a continuous approximation to a graph. As illustrated in Fig. 1, a tree-like graphs can be considered as a discrete approximation to a hyperbolic manifold; the hyperbolic manifold, in turn, can be regarded as a continuous approximation to a tree-like graph.

Menglin Yang and Irwin King were with the Department of Computer Sciences and Engineering, The Chinese University of Hong Kong, Hong Kong SAR, China. Min Zhou and Lujia Pan were with Noah’s Ark Lab, Huawei Technologies, Shenzhen, China.

Correspondence to: Menglin Yang (mlyang@cse.cuhk.edu.hk) and Min Zhou (zhoumin27@huawei.com).

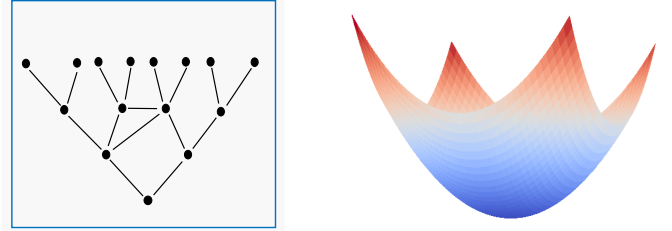


Fig. 1. The (tree-like) graph G in the left subfigure can be considered as a discrete approximation to the (hyperbolic) manifold \mathcal{M} in the right subfigure; on the other hand, the manifold \mathcal{M} can also be approximated as the graph G .

In this work, we concentrate on hyperbolic geometric learning on tree-like graphs. Tree-like graphs are hierarchical-structured or scale-free¹, which widely exists in real-world, such as social networks, recommender systems, world wide web, airline networks, disease-spreading network, etc. Hyperbolic space is a continuous space with exponential volume growth property, producing much more capacity for embeddings [9], [10]. On the other hand, it can well capture the implicit tree-like structure, e.g., hierarchies, power-law distribution. However, real-world graphs are inherently complicated and heterogeneous, and the graphs with overall tree-like structure (e.g., telecommunication network as illustrated in Fig. 2) often include a plethora of intricate substructures as well.

As we know, in geometric learning, the quality of embedding in geometric learning is determined by how well the embedding space fits the intrinsic graph structure [11]. Directly embedding a heterogeneous structure into an homogeneous manifold inevitably leads to structural inductive biases and high distortions. Fortunately, both the embedding space and the graph topology are parametrized by *curvature*, with embedding space curvature being continuous and global and the graph curvature being discrete and local.

In Riemannian geometry, curvature describes the deviation of a geometric object from being flat, such as a straight line or a surface deviates from being a plane, which is originally defined on the continuous smooth manifold. The smooth manifold with positive, zero and negative curvature are spherical, Euclidean and hyperbolic space, respectively. The curvature has also been generalized to discrete objects, like graphs. For graphs, the curvature describes a local pair of neighborhoods deviating from a “flat” case, namely, a grid. The local structure, as shown in Fig. 3 with negative, zero and positive curvature indicate tree-like, flat and cyclic

¹A scale-free graph is that its degree distribution follows a power law, at least asymptotically.

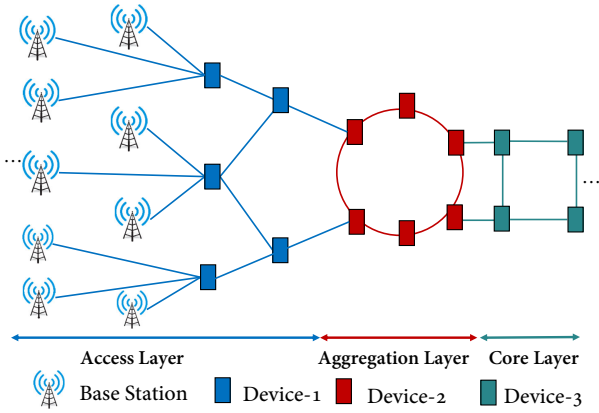


Fig. 2. A real-world telecommunication network. The network receives a large number of messages from the base station in different places at the access layer, and further goes to the aggregation layer and core layer. The overall topology is tree-like with obvious hierarchies, but some local areas are grid or circular.

areas, respectively. Overall, curvature determines the geodesic dispersion, i.e., whether geodesics starting at nearby points with ‘same’ velocity remain parallel (zero curvature), converge (positive curvature), or diverge (negative curvature). This motivates us to seek a solution uniting the discrete into the continuous curvature to acquire higher quality embeddings.

There are several definitions of discrete curvature for graphs, Ollivier Ricci curvature [12], Forman curvature [13]. Most of them are derived on the discretization of Ricci curvature², which shares many properties with the continuous one. It controls the amount of overlap of two distance balls in terms of their radii and the distance between their centers [14], and the lower bound on the Ricci curvature allow one to extract global geometric and topological information [15]. Besides, it is a natural indicator to measure tree-like, flat, and cyclic areas, which makes it comfortable to be integrated into the hyperbolic space to perceive the asymmetries, biases, and hierarchies.

Considering the large capacity of hyperbolic space and the intricate structure of a real-world graph, we present a novel and effective framework, Hyperbolic Curvature-aware Graph Neural Network (HCGNN). In particular, HCGNN utilizes the discrete Ricci curvature to lead message passing of the surroundings and adaptively adjust the global continuous hyperbolic curvature simultaneously. We further theoretically justify the effectiveness of HCGNN as it generates more distant embeddings for the nodes with smaller discrete curvature, and vice versa. Experiments carried on diverse datasets and tasks verify the superiority of HCGNN as it consistently outperforms baselines with large margins. To summary, the main contributions are as follows:

- We design a novel hyperbolic geometric learning framework that encapsulates the graph structure into the continuous embedding space, producing less distortion, powerful expressiveness, and topology-aware embeddings;
- We present a new message technique for hyperbolic

²Ricci curvature is a quantity derived from the second derivatives of the metric tensor

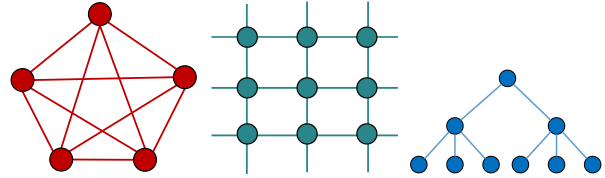


Fig. 3. Examples of cluster, grid and tree-like structure (from left to right). The corresponding graph curvatures are positive, zero and negative, respectively.

graph embedding, and we further prove that it produces a smaller (larger) embedding distance when larger (smaller) curvature is involved, which well handle the inconsistency between the local structure and global curvature of embedding space.

- Extensive experiments show that our proposed model HCGNN achieves significant improvements over various baselines on link prediction and node classification tasks.

II. RELATED WORK

A. Graph Neural Networks (GNNs)

GNNs have gained increasing attention in the field of geometric machine learning, which aim to learn a representation parameterized by neural networks that map graph-structured data into low dimensional space. GNNs have made various achievements in node classification, link prediction, graph reconstruction, etc. [1], [3], [2], [16], [17], [18], [19], [20], [21], [22], [23] However, GNNs generally embed nodes into a Euclidean space, which leads to a large distortion for the dataset with a tree-like and implicitly hierarchical structure.

B. Hyperbolic Geometry

Hyperbolic geometry has also received increasing interest in machine learning and network science communities given its attractive properties. It has been applied to neural networks, for problems of computer vision [24], natural language processing [5], [6], [25], [26], recommender systems [27], [28], [29], [30], [31] and graph embedding tasks [25], [32], [9], [10], [33], [34]. In the graph embedding field, recent works, including HGNN [10], HGCN [9], and HGAT [32] generalize the hyperbolic graph operations on the tangent space. Some others are performed directly in hyperbolic space by properly designing or deriving the neighborhood aggregation ways [35], [36]. Besides, works in [37], [38], [39] and [40] mix different embedding spaces to learn graph embeddings. But most of these methods ignore the local heterogeneous structure of graphs, which cause much distortion.

C. Discrete Graph Ricci Curvatures

Discrete graph Ricci curvatures have been introduced in the network communities for either network alignment [41], network vulnerability or congestion detection [42], [43], community detection [44], [45], or robustness analysis [46], [47] tasks. More recently, curvature graph neural network (CurvGN) [48] introduces Ricci curvature into the realm of graph embedding. In [49], they showed that the edges with

TABLE I
SUMMARY OF OPERATIONS IN THE POINCARÉ BALL MODEL AND THE LORENTZ MODEL ($K < 0$)

	Poincaré Ball	Lorentz Model
Induced distance	$d_B^K(\mathbf{x}, \mathbf{y}) = \frac{1}{\sqrt{ K }} \cosh^{-1} \left(1 - \frac{2K\ \mathbf{x}-\mathbf{y}\ _2^2}{(1+K\ \mathbf{x}\ _2^2)(1+K\ \mathbf{y}\ _2^2)} \right)$	$d_L^K(\mathbf{x}, \mathbf{y}) = \frac{1}{\sqrt{ K }} \cosh^{-1} (K\langle \mathbf{x}, \mathbf{y} \rangle_{\mathcal{L}})$
Logarithmic map	$\log_{\mathbf{x}}^K(\mathbf{y}) = \frac{2}{\sqrt{ K \lambda^K}} \tanh^{-1} \left(\sqrt{ K } \frac{\ \mathbf{x} \oplus_K \mathbf{y}\ _2}{\ \mathbf{x} \oplus_K \mathbf{y}\ _2} \right)$	$\log_{\mathbf{x}}^K(\mathbf{y}) = \frac{\cosh^{-1}(K\langle \mathbf{x}, \mathbf{y} \rangle_{\mathcal{L}})}{\sinh(\cosh^{-1}(K\langle \mathbf{x}, \mathbf{y} \rangle_{\mathcal{L}}))} (\mathbf{y} - K\langle \mathbf{x}, \mathbf{y} \rangle_{\mathcal{L}} \mathbf{x})$
Exponential map	$\exp_{\mathbf{x}}^K(\mathbf{v}) = \mathbf{x} \oplus_K \left(\tanh \left(\sqrt{ K } \frac{\lambda^K \ \mathbf{v}\ _2}{2} \right) \frac{\mathbf{v}}{\sqrt{ K } \ \mathbf{v}\ _2} \right)$	$\exp_{\mathbf{x}}^K(\mathbf{v}) = \cosh \left(\sqrt{ K } \ \mathbf{v}\ _{\mathcal{L}} \right) \mathbf{x} + \mathbf{v} \frac{\sinh(\sqrt{ K } \ \mathbf{v}\ _{\mathcal{L}})}{\sqrt{ K } \ \mathbf{v}\ _{\mathcal{L}}}$
Parallel transport	$PT_{\mathbf{x} \rightarrow \mathbf{y}}^K(\mathbf{v}) = \frac{\lambda_{\mathbf{x}}^K}{\lambda_{\mathbf{y}}^K} \text{gyr}[\mathbf{y}, -\mathbf{x}]\mathbf{v}$	$PT_{\mathbf{x} \rightarrow \mathbf{y}}^K(\mathbf{v}) = \mathbf{v} - \frac{K\langle \mathbf{y}, \mathbf{v} \rangle_{\mathcal{L}}}{1+K\langle \mathbf{x}, \mathbf{y} \rangle_{\mathcal{L}}} (\mathbf{x} + \mathbf{y})$

negative curvature are accountable for the over-squashing problem. In this work, we further explore the possible impetus of discrete graph curvature in hyperbolic geometric learning.

III. BACKGROUND

In this part, we first briefly review necessary definitions of differential geometry, primarily concentrating on hyperbolic geometry. A thorough and in-depth explanation can be found in [50]. We also give a short introduction about Ollivier Ricci curvature, which is a generalized Ricci curvature tailored for discrete object (e.g., graphs). The readers may refer to [12] for more details.

A. Riemannian Geometry

Manifold and Tangent Space. Riemannian geometry is a branch of differential geometry that involves a smooth manifold \mathcal{M} with a Riemannian metric g . An n -dimensional manifold (\mathcal{M}, g) is a real and smooth space, a generalization of a 2-D surface with high dimensions, and can be locally approximated by \mathbb{R}^n . For each point \mathbf{x} in \mathcal{M} , a tangent space $\mathcal{T}_{\mathbf{x}}\mathcal{M}$ is defined as the first-order approximation of \mathcal{M} around \mathbf{x} , which is an n -dimension vector space and isomorphic to \mathbb{R}^n . The Riemannian manifold metric g assigns a smoothly varying positive definite inner product $\langle \cdot, \cdot \rangle: \mathcal{T}_{\mathbf{x}}\mathcal{M} \times \mathcal{T}_{\mathbf{x}}\mathcal{M} \rightarrow \mathbb{R}$ on the tangent space, which allows us to define several geometric properties, such as geodesic distances, angles, and curvature.

Geodesics and Induced Distance Function. For a curve $\gamma: [\alpha, \beta] \rightarrow \mathcal{M}$, the shortest length of γ , i.e., geodesics, is defined as $L(\gamma) = \int_{\alpha}^{\beta} \|\gamma'(t)\|_g dt$. Then the distance of $\mathbf{u}, \mathbf{v} \in \mathcal{M}$, $d^{\mathcal{M}}(\mathbf{u}, \mathbf{v}) = \inf L(\gamma)$ where γ is a curve that $\gamma(a) = \mathbf{u}, \gamma(b) = \mathbf{v}$.

Maps and Parallel Transport. The maps define the relationship between the hyperbolic space and the corresponding tangent space. For a point $\mathbf{x} \in \mathcal{M}$ and vector $\mathbf{v} \in \mathcal{T}_{\mathbf{x}}\mathcal{M}$, there exists a unique geodesic $\gamma: [0, 1] \rightarrow \mathcal{M}$ where $\gamma(0) = \mathbf{x}, \gamma'(0) = \mathbf{v}$. The exponential map $\exp_{\mathbf{x}}: \mathcal{T}_{\mathbf{x}}\mathcal{M} \rightarrow \mathcal{M}$ is defined as $\exp_{\mathbf{x}}(\mathbf{v}) = \gamma(1)$ and logarithmic map $\log_{\mathbf{x}}$ is the inverse of $\exp_{\mathbf{x}}$. The parallel transport $PT_{\mathbf{x} \rightarrow \mathbf{y}}: \mathcal{T}_{\mathbf{x}}\mathcal{M} \rightarrow \mathcal{T}_{\mathbf{y}}\mathcal{M}$ achieves the transportation from point \mathbf{x} to \mathbf{y} that preserves the metric tensors.

Hyperbolic Models. Hyperbolic geometry is a Riemannian manifold with a constant negative curvature. There exist multiple equivalent hyperbolic models which show different characteristics but are mathematically equivalent. We here

mainly consider two widely studied hyperbolic models: the Poincaré ball model [5] and the Lorentz model (also known as the hyperboloid model) [6]. Let $\|\cdot\|$ be the Euclidean norm and $\langle \cdot, \cdot \rangle_{\mathcal{L}}$ denote the Minkowski inner product, respectively. The two models are given by Definition III.1 and Definition III.2, respectively. The related formulas and operations, e.g., distance, maps, and parallel transport are further summarized in TABLE I, where \oplus_K and $\text{gyr}[\cdot, \cdot]v$ are Möbius addition [51] and gyration operator [51], respectively.

Definition III.1 (Poincaré Ball Model). *The Poincaré ball model with negative curvature K is defined as a Riemannian manifold (\mathcal{B}_K^n, g_B) , where $\mathcal{B}_K^n = \{\mathbf{x} \in \mathbb{R}^n : \|\mathbf{x}\|_2^2 < -1/K\}$ is an open n -dimensional ball with radius $1/\sqrt{|K|}$. Its metric tensor $g_B = \lambda^2 g_E$, where $\lambda = \frac{2}{1+K\|\mathbf{x}\|_2^2}$ is the conformal factor and $g_E = I_n$ is the Euclidean metric.*

Definition III.2 (Lorentz Model). *The Lorentz model (also named hyperboloid model) with negative curvature K is defined as the Riemannian manifold (\mathcal{L}_K^n, g_L) , where $\mathcal{L}_K^n = \{\mathbf{x} \in \mathbb{R}^{n+1} : \langle \mathbf{x}, \mathbf{x} \rangle_{\mathcal{L}} = \frac{1}{K}\}$ and $g_L = \text{diag}([-1, 1, \dots, 1])$.*

B. Graph Curvature

Curvature is a fundamental concept in smooth spaces which has also generalized to discrete objects (e.g., graphs). There are several distinct notions of discrete Ricci curvature for graphs or networks, such as the Forman-Ricci curvature [13] and Ollivier-Ricci curvature (ORC) [12]. Here we mainly focus on ORC since it is more geometrical [12], [14]. Another reason is ORC builds a bridge between continuous geometry and discrete structures [52], [53].

Definition III.3 (Ollivier-Ricci Curvature). *Let $G = (V, E)$ be a locally finite, connected, and simple graph (i.e., G contains no multiple edges or self loops), for any two distinct vertices x_1, x_2 , the ORC of x_1 and x_2 is defined as*

$$\kappa(v_1, v_2) = 1 - \frac{W(m_{v_1}, m_{v_2})}{d(v_1, v_2)} \in (-2, 1), \quad (1)$$

where $d(v_1, v_2)$ is the shortest path between v_1 and v_2 on graph G , $W(m_{v_1}, m_{v_2})$ is the Wasserstein distance (see Definition III.4) between two probability measures (see Definition III.5) m_{v_1} and m_{v_2} .

Definition III.4 (Wasserstein Distance). Let m_1, m_2 be two probability measures on V . The Wasserstein distance $W(m_1, m_2)$ between m_1 and m_2 is given by

$$W(m_1, m_2) = \inf_{\pi_{i,j} \in \Pi} \sum_{v_i, v_j \in V} \pi_{i,j}(v_i, v_j) d(v_i, v_j), \quad (2)$$

where $\pi_{i,j} : V \times V \rightarrow [0, 1]$ is a transport plan, i.e., the probability measure of the amount of mass transferred from v_i to v_j . Then to seek an optimal transference plan (π) that is to minimize the total cost of moving from v_i to v_j such that for every v_i, v_j in V satisfying

$$\sum_{v_i \in V} \pi_{i,j}(v_i, v_j) = m_1; \sum_{v_j \in V} \pi_{i,j}(v_i, v_j) = m_2. \quad (3)$$

Definition III.5 (Probability Measure). Given $G = (V, E)$, for a vertex v_i in V , denote d_{v_i} the degree of $v \in V$ and $N(v)$ the neighbors of v , for any $p \in [0, 1]$, the probability measure m_{v_i} on V is defined as:

$$m_{v_i} = \begin{cases} p, & \text{if } v = v_i \\ \frac{1-p}{d_v}, & \text{if } (v_i) \in N(v). \\ 0, & \text{otherwise} \end{cases} \quad (4)$$

Geometric intuition. ORC seeks the most efficient transportation plan that preserves mass between two probability measures, which may be solved using linear programming. Intuitively, transporting messages between two nodes whose neighbors are highly overlapping, such as two nodes in the same cluster, is costless. On the other hand, if two nodes are situated in distinct groups or clusters, information flow between them is difficult.

IV. METHODOLOGY

Our approach HCGNN exploits the integration of discrete and continuous curvature to enhance hyperbolic geometric learning. The basic idea is to *enlarge the message flow when the local graph structure well matches the hyperbolic space and reduce the message prorogation when the local structure is incompatible with the embedding space*. Thereby curvature guidance can help the hierarchical formation and reduce the incompatible distortion. We detail the two key components: Hyperbolic Curvature-aware Message Propagation (HCMP) and ORC based Homophily Constraint (OHC) in below. For brevity, we use \mathcal{H} to denote the case that is applicable for both Poincaré ball model and Lorentz model.

A. Hyperbolic Curvature-aware Message Propagation (HCMP)

HCMP is the core to achieve the connection between graph topology and the embedding in hyperbolic space, which mainly consists of three operations as works in [1], [9], i.e., feature transformation, message aggregation, and nonlinear activation.

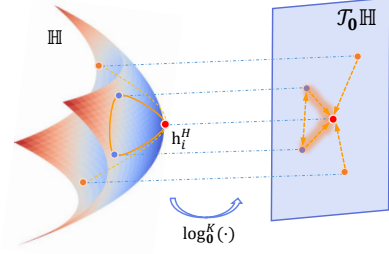


Fig. 4. Illustration of the proposed Curvature-aware aggregation. Compared with the traditional aggregation scheme, the proposed method further makes the aggregation process aware of the local structure.

1) *Hyperbolic Feature Transformation:* Hyperbolic feature transformation is formulated as:

$$\mathbf{h}_i^{\ell, \mathcal{H}} = \left(\mathbf{W}^\ell \otimes^{K_{\ell-1}} \mathbf{x}_i^{\ell-1, \mathcal{H}} \right) \oplus^{K_{\ell-1}} \mathbf{b}^\ell, \quad (5)$$

where ℓ denotes the ℓ -th layer, \mathbf{W} is the trainable matrix and \mathbf{b} is the bias. $\mathbf{W} \otimes^K \mathbf{x} := \exp_{\mathbf{o}}^K(\mathbf{W} \log_{\mathbf{o}}^K(\mathbf{x}))$ and $\mathbf{x} \oplus^K \mathbf{b} := \exp_{\mathbf{x}}^K(PT_{\mathbf{o} \rightarrow \mathbf{x}}^K(\mathbf{b}))$ are matrix-vector multiplication and bias translation operations in hyperbolic space, respectively. The superscript \mathcal{H} denotes the hyperbolic feature.

2) *Hyperbolic Curvature-Aware Aggregation:* Hyperbolic Curvature-Aware Aggregation (CA), as shown in Figure 5, is built in the tangent space of the origin:

$$\tilde{\mathbf{h}}_i^{\ell, \mathcal{H}} = \exp_{\mathbf{o}}^{K_{\ell-1}} \left(\sum_{j \in \mathcal{N}_i} \tilde{\kappa}_{i,j} \cdot \log_{\mathbf{o}}^{K_{\ell-1}}(\mathbf{h}_j^{\ell, \mathcal{H}}) \right). \quad (6)$$

Here $\tilde{\kappa}_{i,j}$ is the hyperbolic level-aware curvature, computed by softmax operation within the neighbors \mathcal{N}_i (\mathcal{N}_i contains the node self):

$$\tilde{\kappa}_{i,j} = \text{softmax}_{j \in \mathcal{N}(i)} (\text{MLP}(\kappa_{i,j} - |L_i - L_j|)), \quad (7)$$

where $\kappa_{i,j}$ is the raw ORC value, L_i and L_j are scalar representing the hyperbolic distance (c.f. TABLE I) of point i and j to the origin \mathbf{o} , respectively, which can be regarded as the node level. $|L_i - L_j|$ indicates the absolute level difference. It is easy to know that the hyperbolic level-aware curvature $\tilde{\kappa}_{i,j}$ decreases if two linked nodes (i, j) have large level differences in hyperbolic space. When it comes to the case where the topology information and node features are inconsistent to a certain degree, e.g., the network is quite sparse or depends more on the node features, we propose a feature-attention enhanced aggregation (CURVATT), which encodes node state into the hyperbolic level-aware curvature:

$$\tilde{\kappa}'_{i,j} = \frac{w_\kappa \tilde{\kappa}_{i,j} + w_\alpha \alpha_{i,j}}{w_\kappa + w_\alpha}, \quad (8)$$

where $\alpha_{i,j}$ is hyperbolic feature attention, w_κ and w_α are the trainable parameters that adjust structure information and feature correlation with the initial value 1.0. The hyperbolic feature attention $\alpha_{i,j}$ is defined as:

$$\alpha_{i,j} = \text{softmax}_{j \in \mathcal{N}_i} \left(\text{MLP}(\log_{\mathbf{o}}^K(\mathbf{h}_i^{\mathcal{H}}) \| \log_{\mathbf{o}}^K(\mathbf{h}_j^{\mathcal{H}})) \right). \quad (9)$$

3) *Hyperbolic Non-linear Activation*: After that, we apply a nonlinear activation:

$$\mathbf{x}_i^{\ell, \mathcal{H}} = \sigma^{K_{\ell-1}, K_{\ell}}(\tilde{\mathbf{h}}^{\ell, \mathcal{H}}) = \exp_{\circ}^{K_{\ell}} \left(\sigma(\log_{\circ}^{K_{\ell-1}}(\tilde{\mathbf{h}}^{\ell, \mathcal{H}})) \right). \quad (10)$$

Geometric intuition. The real-world networks are with heterogeneous local structures and distortions are inevitable if we directly embed them into a homogeneous manifold. For instance, the embedding of quasi-cycle graphs such as $n \times n$ square lattices (zero curvature) and n -node cycles (positive curvature) incur at least a multiplicative distortion of $O(n/\log n)$ in hyperbolic space [54]. Graph curvature is able to mitigate this distortion. The geometric intuition is that the more positive the Ricci curvature is, the more two distance balls centered at nearby points overlap, and therefore, the cheaper it is to transport the mass from one to the other. Theoretical results show that with the increasing number of triangles involved in the linked pair (i, j) , the lower bound of curvature will be increased [14], as stated in Theorem IV.1. It is easy to understand because when the two vertices share many triangles, then the transportation distance should be smaller, and the curvature, therefore, is correspondingly larger.

Theorem IV.1 (Lower bound of ORC). [14] *On a locally finite graph, for any pair of neighboring vertices i, j , let $\#(i, j) :=$ number of triangles which include i, j as vertices for $i \sim j$. Then, we have the inequality, saying that*

$$\kappa_{i,j} \geq - \left(1 - \frac{1}{d_i} - \frac{1}{d_j} - \frac{\#(i,j)}{d_i \wedge d_j} \right)_+ + \left(1 - \frac{1}{d_i} - \frac{1}{d_j} - \frac{\#(i,j)}{d_i \vee d_j} \right)_+ + \frac{\#(i,j)}{d_i \vee d_j}, \quad (11)$$

where $s_+ := \max(s, 0)$, $s \vee t := \max(s, t)$, and $s \wedge t := \min(s, t)$.

Proposition IV.1 further demonstrates the relations of ORC and embedding distance, i.e., when a large curvature is involved within the linked node, the closer of their embedding distance using HCMP, which thus mitigates the distortion.

Proposition IV.1 (Embedding Distance w.r.t ORC). *Let $(i, j) \in E$ be the linked pair, $\mathbf{h}_i, \mathbf{h}_j \in \mathbb{R}^d$ be the node state in the tangent space, d_i be the degree of node i , and D be the distance of node i and node j in the tangent space, that is*

$$\mathbf{D} = \|\mathbf{h}_i - \mathbf{h}_j\| \quad (12)$$

where $\|\cdot\|$ is the Euclidean norm. Define a large ORC as $\tilde{\kappa}_{i,j} > \max\{1/d_i, 1/d_j\}$ and a small ORC as $\tilde{\kappa}_{i,j} < \min\{1/d_i, 1/d_j\}$. Then, when the large ORC is involved, their embedding distance will get smaller if using HCMP. On the contrary, when the small ORC is involved, their embedding distance will get larger.

Proof. In the following, we use \mathbf{D}_l and \mathbf{D}_s to denote the distance when large and small curvature $\tilde{\kappa}$ are involved, respectively. The main idea is that when there is a large curvature involved, the node distance will be decreased compared with the original case, that is $\mathbf{D}_l < \mathbf{D}$. At the same time, when there

is a small curvature involved, the node distance will increase, that is $\mathbf{D}_s > \mathbf{D}$.

(1) When a large curvature (i.e., $\kappa_{i,j} > \max(1/d_i, 1/d_j)$) is involved, more message will be transferred, and we decompose the embedding, taking \mathbf{h}_i as an example, into two components: one is from original \mathbf{h}_i and another is the incremental parts from \mathbf{h}_j , then

$$\begin{aligned} \mathbf{D}_l &= \|(\mathbf{h}_i + \alpha_i \mathbf{h}_j) - (\mathbf{h}_j + \alpha_j \mathbf{h}_i)\| \\ &= \|(\mathbf{h}_i - \alpha_j \mathbf{h}_i) - (\mathbf{h}_j - \alpha_i \mathbf{h}_j)\|, \end{aligned} \quad (13)$$

where α_i (α_j) is the difference between $\tilde{\kappa}_{i,j}$ and $1/d_i$ ($1/d_j$), i.e., $\alpha_i = \tilde{\kappa}_{i,j} - 1/d_i$, $\alpha_j = \tilde{\kappa}_{i,j} - 1/d_j$. Since $\tilde{\kappa}_{i,j} > \max(1/d_i, 1/d_j)$, α_i and α_j are both positive. Let $\alpha_{ij} = \alpha_i \approx \alpha_j$, then

$$\begin{aligned} \mathbf{D}_l &\approx \|(\mathbf{h}_i - \alpha_{ij} \mathbf{h}_i) - (\mathbf{h}_j - \alpha_{ij} \mathbf{h}_j)\| \\ &= (1 - \alpha_{ij}) \|\mathbf{h}_i - \mathbf{h}_j\| \\ &< \mathbf{D}. \end{aligned} \quad (14)$$

Then, we easily know that when large curvature is involved, the distance will be reduced and two nodes will be closer to each other. What's more, the larger the curvature, the closer the nodes are.

(2) Similarly, when a small curvature ($\kappa_{i,j} < \min(1/d_i, 1/d_j)$) is involved, less messages will be transferred, and we decompose the embedding, taking \mathbf{h}_i as an example, into two components: one is from original \mathbf{h}_i and another is the reduction parts of \mathbf{h}_j , that is

$$\begin{aligned} \mathbf{D}_s &= \|(\mathbf{h}_i - \beta_i \mathbf{h}_j) - (\mathbf{h}_j - \beta_j \mathbf{h}_i)\| \\ &\approx (1 + \beta_{ij}) \|\mathbf{h}_i - \mathbf{h}_j\| \\ &> \mathbf{D}, \end{aligned} \quad (15)$$

where β_i is the difference between $1/d_i$ and $\tilde{\kappa}_{i,j}$, i.e., $\beta_i = 1/d_i - \tilde{\kappa}_{i,j}$, $\beta_j = 1/d_j - \tilde{\kappa}_{i,j}$. Both β_i and β_j are positive in that $\kappa_{i,j} < \min(1/d_i, 1/d_j)$. Let $\beta_{ij} = \beta_i \approx \beta_j$, then, we easily know that when small curvature is involved, the node pair will become more distant in the embedding space. What's more, the smaller the curvature, the more distant the nodes are. \square

B. ORC Homophily Constraint (OHC)

In the degree-based learning paradigm, like GCN [1], the influence of a node on another node decays exponentially as their graph distance increases as shown by [55]. In the hyperbolic message passing learning paradigm, including the proposed HCMP, it also shows a similar phenomenon, which causes too much influence loss in long-term propagation. Especially, if the paths consist of numerous connections to other nodes, the node influence is minimal.

Theorem IV.2 (Decaying property of HCMP). *Let p be a path between node u and node v , d_g^* be the shortest distance between u and v , let C be a constant. Consider the node influence $I_{u,v}$ from v to u using HCMP, $I_{u,v} \leq C\gamma^{d_g^*}$ ($0 < \gamma \leq 1$). The condition for equality is $d_g^* = 1$, and v is the unique neighbors of node u , correspondingly $C = 1, \gamma = 1$.*

Proof. Recall the aggregation rule in Equations (6) and (7), we focus on the aggregation in the tangent space and ignore

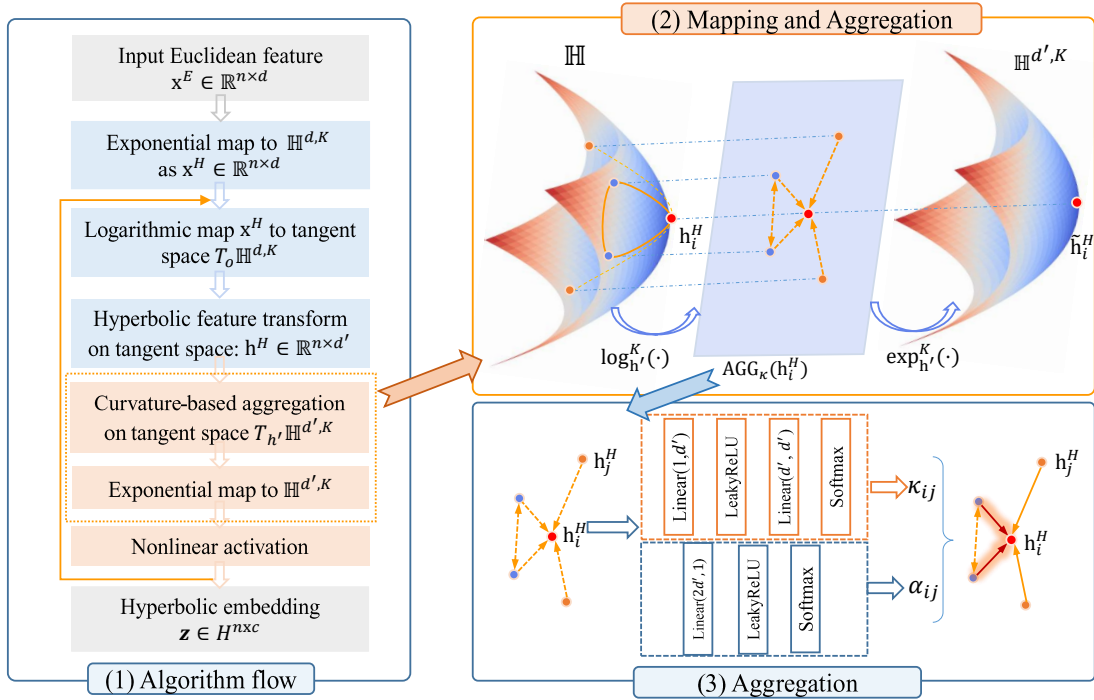


Fig. 5. Illustration of the proposed Curvature-aware aggregation. Compared with the traditional aggregation scheme, the proposed method further makes the aggregation process aware of the local structure.

the previous logarithmic map and the later exponential map since they are applied before and after the whole aggregation process, respectively. Besides, the level difference is a scalar computed according to the distance of one node to the origin, which is detached from the trainable variable in settings. Then for any node u and v , the update rule in the tangent space can be formulated as:

$$\mathbf{z}_u = \sum_{j \in \mathcal{N}(u)} \tilde{\kappa}_{u,j} \mathbf{z}_j = \frac{1}{K_{uu}} \sum_{j \in \mathcal{N}(u)} \exp(\tilde{\kappa}_{u,j}) \mathbf{z}_j, \quad (16)$$

where $K_{uu} = \sum_{j \in \mathcal{N}(u)} \exp(\tilde{\kappa}_{u,j})$. By an expansion of node in the neighbor $\mathcal{N}(j)$, we have:

$$\mathbf{z}_u = \frac{1}{K_{uu}} \sum_{j \in \mathcal{N}(u)} \exp(\tilde{\kappa}_{u,j}) * \frac{1}{K_{jj}} \sum_{k \in \mathcal{N}(j)} \exp(\tilde{\kappa}_{j,k}) \mathbf{z}_k. \quad (17)$$

We completely expand it:

$$\mathbf{z}_u = \frac{1}{K_{uu}} \sum_{j \in \mathcal{N}(u)} \exp(\tilde{\kappa}_{u,j}) * \dots * \frac{1}{K_{oo}} \sum_{p \in \mathcal{N}(o)} \exp(\tilde{\kappa}_{o,p}) \mathbf{z}_p. \quad (18)$$

Node influence $I_{u,v}$ of v on u in the message passing output is $I_{u,v} = \|\partial \mathbf{z}_u / \partial \mathbf{z}_v\|$, where the norm is any subordinate norm and the node influence measures how a change in v passes to a change in u . By equation (18), the node influence can be computed as:

$$\begin{aligned} I_{u,v} &= \left\| \frac{\partial \mathbf{z}_u}{\partial \mathbf{z}_v} \right\| \\ &= \left\| \frac{\partial}{\partial \mathbf{z}_v} \left(\frac{1}{K_{uu}} \sum_{j \in \mathcal{N}(u)} \exp(\tilde{\kappa}_{u,j}) * \dots * \frac{1}{K_{oo}} \sum_{p \in \mathcal{N}(o)} \exp(\tilde{\kappa}_{o,p}) \mathbf{z}_p \right) \right\| \end{aligned} \quad (19)$$

The partial derivative of the nodes in Equation (19) is zero if they are not on the path between node u and v , and then the

feature influence can be decomposed into the sum influence of all related paths. Suppose there are n paths between u and v , then

$$I_{u,v} = \left\| \frac{\partial}{\partial \mathbf{z}_v} (I_{p_1} + \dots + I_{p_i} \dots + I_{p_n}) \right\|, \quad (20)$$

where

$$I_{p_i} = \frac{1}{K_{uu}} \exp(\tilde{\kappa}_{u,p_i^i}) \dots \underbrace{\frac{1}{K_{p_{n_i}^i p_{n_i}^i}} \exp(\tilde{\kappa}_{p_{n_i}^i, v})}_{S(I_{p_i})} \mathbf{z}_v.$$

Note that, in Equation (20), the scalar term $S(I_{p_i})$ ranges from $(0, 1]$ and all I_{p_i} ($1 \leq i \leq n$) have the term m_v , thus we separate $S(I_{p_i})$ and the rest derivative term and then uses the absolute homogeneous property, i.e., $\|\alpha M\| = |\alpha| \|M\|$

$$\begin{aligned} I_{u,v} &= |S(I_{p_1}) + \dots + S(I_{p_i}) \dots + S(I_{p_n})| \left\| \frac{\partial \mathbf{z}_v}{\partial \mathbf{z}_v} \right\| \\ &= |S(I_{p_1}) + \dots + S(I_{p_i}) \dots + S(I_{p_n})| \\ &\leq |n * \max(S(I_{p_i}))| \end{aligned} \quad (21)$$

$$\begin{aligned} &= |n * \gamma^n| \\ &\leq |n * \gamma^{d_g^*}| \\ &= C \gamma^{d_g^*}, \end{aligned}$$

where d_g is the shortest path between u and v , $d_g^* \leq n^i$ and $0 < \gamma \leq 1$, thus the second inequality holds on in Equation (21). For more generality, we use constant C to denote the n . The condition for equality is if and only if $d_g^* = 1$ and the v is the unique neighbor of node u , i.e., $\gamma = 1$ and $C = 1$. \square

Theorem IV.2 shows that the node influence using HCOMP exponentially decays as the shortest graph distance d_g^* between

TABLE II

PROFILING EVALUATION ON NODE CLASSIFICATION. F1-SCORE WITH STANDARD DEVIATION FOR DISEASE AND AIRPORT; ACCURACY FOR OTHERS (THE HIGHER, THE BETTER).

DATASET Hyperbolicity (δ)	DISEASE 0	AIRPORT 1	PUBMED 3.5	CORA 11
EUC	32.5 \pm 1.1	60.9 \pm 3.4	48.2 \pm 0.7	23.8 \pm 0.7
HYP [5]	45.5 \pm 3.3	70.2 \pm 0.1	68.5 \pm 0.3	22.0 \pm 1.5
GCN [1]	69.7 \pm 0.4	81.4 \pm 0.6	78.1 \pm 0.2	81.3 \pm 0.3
GAT [2]	70.4 \pm 0.4	81.5 \pm 0.3	79.0 \pm 0.3	83.0 \pm 0.7
SAGE [56]	69.1 \pm 0.6	82.1 \pm 0.5	77.4 \pm 2.2	77.9 \pm 2.4
SGC [57]	69.5 \pm 0.2	80.6 \pm 0.1	78.9 \pm 0.0	81.0 \pm 0.1
CurvGN [48]	89.8 \pm 2.9	84.7 \pm 1.5	78.3 \pm 0.3	82.0 \pm 0.9
κ GCN [58]	82.1 \pm 1.1	—	78.3 \pm 0.6	80.8 \pm 0.6
HGCN [9]	74.5 \pm 0.9	90.6 \pm 0.2	80.3 \pm 0.3	79.9 \pm 0.2
LGCN [36]	84.4 \pm 1.0	90.9 \pm 1.0	78.8 \pm 0.5	83.3 \pm 0.5
HCGNN	92.3 \pm 1.4	92.8 \pm 0.4	82.1 \pm 0.5	82.5 \pm 0.6
Δ_E (%)	+31.1	+13.0	+3.9	-0.6
Δ_κ (%)	+2.8	+9.6	+4.9	+0.6
Δ_H (%)	+2.2	+3.6	+5.0	+5.4

two nodes increases.³ In other words, distant nodes in dense areas will have less interaction. To alleviate the phenomenon, we propose an OHC to enhance the connection within linked pairs. The basic idea is to push the embeddings of linked nodes closer if their ORC value is larger than a threshold. In this way, we can enforce disjoint node pairs in dense area or cluster to have more influence on each other through their mutual neighbors, which is given by:

$$l_{hc_+} = \frac{1}{|E_\kappa|} \sum_{(i,j) \in E_\kappa} -\log p(\mathbf{x}_i^{\ell, \mathcal{H}}, \mathbf{x}_j^{\ell, \mathcal{H}}), \quad (22)$$

where E_κ is the filtered edge set based on ORC threshold τ^4 ; $p(\cdot)$ is Fermi-Dirac function, indicating the probability of two hyperbolic nodes (u, v) link or not, which is given by:

$$p(\mathbf{x}_u, \mathbf{x}_v) = [\exp(d_{\mathcal{H}}^2(\mathbf{x}_u, \mathbf{x}_v) - r)/t + 1]^{-1}, \quad (23)$$

and $d_{\mathcal{H}}(\mathbf{x}_u, \mathbf{x}_v)$ is the hyperbolic distance from u to v , r and t is hyper parameters. We also sample the same number of negative link pairs. Totally, $l_{hc} = l_{hc_+} + l_{hc_-}$.

Geometric intuition. HCMP helps build the connection between the graph topology and the embedding space, adjust the curvature of the hyperbolic geometry, and guide the information flow. It also shortens the distance of two linked nodes in an area with many triangles, helping mitigate the distortion caused by hyperbolic space. Nonetheless, HCMP is local inherently, and the proposed OHC further enhances the interactions of unconnected nodes, which is non-local.

C. HCGNN Architecture

Given the Euclidean feature \mathbf{x}^E , we first project it into the hyperbolic manifold by the exponential map. HCGNN architecture takes layers of HCMP as the encoder. Following the literature, the Fermi-Dirac function is used as a decoder in the link prediction task. For the node classification task, the

³This conclusion can also be easily extended to other message passing fashion in hyperbolic space.

⁴We select edges if their ORC value is larger than 0.

TABLE III

PROFILING EVALUATION ON LINK PREDICTION. AUC SCORES WITH STANDARD DEVIATION ARE REPORTED (THE HIGHER, THE BETTER). THE BEST IS BOLD.

DATASET Hyperbolicity(δ)	DISEASE 0	AIRPORT 1	PUBMED 3.5	CORA 11
EUC	60.9 \pm 3.4	92.0 \pm 0.0	83.3 \pm 0.1	82.5 \pm 0.3
HYP [5]	70.2 \pm 0.1	94.5 \pm 0.0	87.5 \pm 0.1	87.6 \pm 0.2
GCN [1]	64.7 \pm 0.5	89.3 \pm 0.4	91.1 \pm 0.5	90.4 \pm 0.2
GAT [2]	69.8 \pm 0.3	90.5 \pm 0.3	91.2 \pm 0.1	93.7 \pm 0.1
SAGE [3]	65.9 \pm 0.3	90.4 \pm 0.5	86.2 \pm 1.0	85.5 \pm 0.6
SGC [57]	65.1 \pm 0.2	89.8 \pm 0.3	94.1 \pm 0.0	91.5 \pm 0.1
CurvGN [48]	80.6 \pm 0.8	89.5 \pm 0.3	91.6 \pm 0.4	72.5 \pm 0.7
κ GCN [58]	92.0 \pm 0.5	—	94.9 \pm 0.3	92.6 \pm 0.4
HGCN [9]	90.8 \pm 0.3	96.4 \pm 0.1	96.3 \pm 0.0	92.9 \pm 0.1
LGCN [36]	96.6 \pm 0.6	96.0 \pm 0.6	96.6 \pm 0.1	93.6 \pm 0.4
HCGNN	96.7 \pm 0.1	98.2 \pm 0.1	96.7 \pm 0.1	95.0 \pm 0.1
Δ_E (%)	+27.2	+8.5	+2.8	+1.4
Δ_κ (%)	+4.1	+9.7	+1.9	+2.6
Δ_H (%)	+0.6	+0.2	+1.3	+1.1

final hyperbolic vector is mapped back to tangent space and decoded with MLP, which is the same with work [9].

V. EXPERIMENTS

A. Experimental Setup

Datasets. The datasets used for evaluation in this work are DISEASE, AIRPORT, and three benchmark citation networks, CITESEER, PUBMED, and CORA. In DISEASE, the label of a node indicates whether the node is infected by a disease or not, and the node features associate the susceptibility to the disease. The disease spreading network has an evident hierarchical structure, which can fully unleash the capacity of hyperbolic embedding models. We use it to verify the further improvements of our proposal. In AIRPORT, each node is an airport, the edge indicates whether there is a route between two airports, and the corresponding label is the population of the country the airport belongs to. For CITESEER, PUBMED, or CORA, each node is a scientific paper characterized by the corresponding bag-of-words representations, edges denote citations and node labels are academic (sub)areas. Compared to DISEASE and AIRPORT, the citation networks are less hierarchical, which are used here to then demonstrate the generalization ability of the proposal.

Baselines. We compare our proposed model with various baselines. (1) *Shallow Euclidean and hyperbolic models*, including Euclidean embeddings (EUC) and Poincaré embeddings (HYP) [5]; (2) *Euclidean GNNs*, i.e., GCN [1], GraphSAGE (SAGE) [3], Graph Attention Networks (GAT) [2], Simplified Graph Convolution, (SGC) [57]; (3) *Curvature-related GNNs*, including Curvature Graph Network (CurvGN) [48] which applies the discrete curvature in Euclidean model and κ GCN which deploys GNNs to products of constant curvature spaces, both of them are close to our work; *Hyperbolic GNNs*, including HGCN [9], HGNN [10], HGAT [32], LGCN [36].

Experimental Details Data split. We evaluate HCGNN on both node classification and link prediction tasks. The data split is the same with the previous works [9]. More specifically,

in link prediction, we randomly split edges into 85%, 5%, 10% for training, validation, and test sets, respectively. For node classification, we split nodes into 70%, 15%, 15% for AIRPORT, 30%, 10%, 60% for DISEASE, and we use 20 labeled train examples per class for CORA, CITESEER, and PUBMED. *Implementation details.* We closely follow the parameter settings as HGCN [9], fix the number of embedding dimensions to 16 and then perform hyper-parameter search on a validation set over learning rate, weight decay, dropout, and the number of layers. We also adopt the early stopping strategies based on validation set as [9]. For baselines, we mainly refer to the reported results in literature, and for the inconsistent cases (such as different embedding dimensions in H2H-GCN), we re-implement their official code in the similar experimental settings. *Evaluation metric.* Following the literature, we report the F1-score for DISEASE and AIRPORT datasets, and accuracy for the others in the node classification tasks. For the link predictions task, the Area Under Curve (AUC) is calculated.

B. Experimental Results

We report the results of 10 random experiments⁵, including standard deviations in TABLE II and III, where the $\Delta_E, \Delta_\kappa, \Delta_H$ is the improvement of the proposed model HCGNN over the Euclidean GNNs, Curvature-related GNNs and Hyperbolic GNNs, respectively.

a) Node Classification: The experimental results of node classification are presented in TABLE II, where a smaller hyperbolicity value indicates the given dataset is more tree-like. The key findings are summarized as follows: (1) Overall, the proposed model performs impressively, surpassing previous models on four out of five datasets. Specifically, hyperbolic models (e.g., HGCN, LGCN) performs substantially better on the more hyperbolic dataset (e.g., DISEASE) than on the less hyperbolic dataset; Euclidean models (e.g., GCN, GAT) find more success on the less hyperbolic datasets (e.g., CORA) than on the more hyperbolic dataset; whereas our model performs better on both datasets, which is consistent with our motivation, namely, that the graph can be better learned under the guidance of curvature. In addition, from the improvements of Δ_κ , we discovered that CurvGN with discrete curvature and κ GCN with continuous curvature both perform worse than our method which validates the power of hyperbolic geometry and the curvature-aware learning. (3) When it comes to CORA, both hyperbolic models and the proposed HCGNN fail to outperform Euclidean GAT [2], indicating Euclidean geometry is more suitable for modeling data with scarcely hierarchical structures. Nevertheless, it is noted that HCGNN still outperforms well-known Euclidean GCN models, e.g., GCN [1], SGC [57], SAGE [3]. It is observed that the proposed method HCGNN also helps to narrow down the gap between hyperbolic models and Euclidean GAT.

b) Link Prediction: The experimental results of link prediction tasks are summarized in TABLE III. In the link prediction task, we further have the following observations:

⁵Due to limited space, the reported results are with Poincaré Ball model and the results on Lorentz model are similar.

TABLE IV
COMPUTATION COST OF RICCI CURVATURE WHERE THE UNIT OF TIME IS SECONDS. NC: NODE CLASSIFICATION; LP: LINK PREDICTION.

TASK	DISEASE	AIRPORT	CITeseer	PUBMED	CORA
NC (s)	0.8	82.6	2.7	72.3	2.3
LP (s)	1.5	46.4	2.5	60.0	2.1

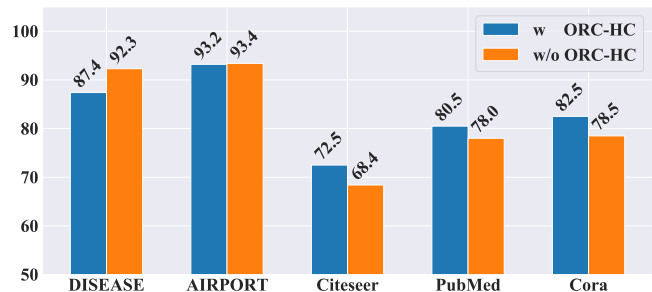


Fig. 6. The performance of node classification by HCGNN with OHC and without OHC.

(1) Compared with Euclidean counterparts, Our proposed HCGNN and other hyperbolic models have achieved better performance. It is because hyperbolic space owns a larger embedding space, where the structural dependencies could be well preserved by the link prediction loss, providing more space or boundary for nodes to be well arranged; (2) In comparison with the advanced hyperbolic models, our model also obtains remarkable gains and refresh the records.

According to the above extensive experiments, we are safe to conclude that equipping ORC into hyperbolic geometry further improves its generalization ability, obtaining high-quality representations for both tree-like and non-tree-like structured data. This confirms our primary motivation that the curvature carries rich information which is beneficial for graph representation learning in the embedding manifold. Specifically, incorporating the structure information featured by ORC helps the models developed in a continuous manifold with negative curvature to perceive the role of each node, accelerating the learning procedure, and reducing the distortion for graph embedding of less hierarchical networks.

VI. ANALYSIS AND DISCUSSION

A. Performance of Aggregations

In section IV-A, we present two tangential aggregation methods: curvature-based (CURV) and feature-enhanced (CURVATT). We further test the two aggregations and results are recorded in TABLE V. As it is seen that the feature-enhanced version yields better results in most cases. This is straightforward as the real-world system is indeed complex, and the node features and topology collected are not always consistent. Our feature-enhanced version then provides a more flexible and learnable way to fusion information of different aspects.

B. Effectiveness of OHC

Figure 6 displays the results of adding OHC or not on HCGNN. As it observed, the performance degenerates sub-

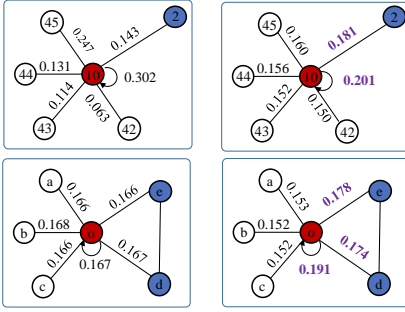


Fig. 7. A tree-like area (upper row) and a triangle-contained area (lower row) with edge weights by HGCN (left column) and HCGNN (right column).

stantially on DISEASE when applying OHC, while there are significant improvements on the three citation networks, i.e., Citeseer, PubMed, and Cora. This phenomenon can be understood as follows. Adding OHC as in node classification will force linked nodes to obtain more similar representations. For the pure tree-like dataset, i.e., DISEASE (without any triangle and circle), these node pairs belong to different levels and adding OHC impair the learning of asymmetric dependencies, which further affects the establishment of hierarchical awareness. When it comes to the citation networks instead, OHC helps to reduce the distortion caused by hyperbolic geometry and thus boost the learning.

C. Case Study of Graph Curvature

We further extract a subtree centered on a given node (taking node 10 as an example) from DISEASE dataset, where node 2 comes from the upper level and other nodes (42, 43, 44, 45) belong to the lower level and the edges indicate disease propagation paths. We further attach the corresponding edge weights of HCGNN and HGCN trained for node classification, respectively, as shown in the upper two sub-figures of Fig. 7. It is observed that HCGNN (the upper right) well distinguishes node levels as it assigns larger weight to the parent node (i.e., node 2) and pays similar attentions to the child nodes from the same level, which is, on the contrary, fail to be perceived by HGCN (the upper left). This validates the role of ORC in guiding hierarchical learning.

Furthermore, we randomly select a subgraph with triangles from the citation network, CORA, as illustrated in the lower two sub-figures of Fig. 7, where nodes $\{o, e, d\}$ compose a triangle. Similarly, we fetch the weights around node o . From the results shown in Fig. 7 (the lower two figures), we easily know that the proposed HCGNN (the lower right) successfully detects the local triangle and assigns larger weights to encourage message exchange. Without surprise, HGCN (the lower left) fails to perceive the dense area. The above observations further validate the efficacy of ORC in finding local clusters and alleviating the distortion caused by hyperbolic geometry.

D. Computational Complexity of ORC

The problem of calculating ORC is broadly formulated as linear programming problems [59], [60] and the computational complexity is $O(|E|d_{\max}^3)$ where d_{\max} is the maximal degree.

TABLE V
PERFORMANCE OF DIFFERENT AGGREGATION METHODS: CURVATURE (CURV) AND FEATURE-ENHANCED CURVATURE (CURVATT).

DATASET	NC		LP	
	CURV	CURVATT	CURV	CURVATT
DISEASE	91.8 \pm 1.9	92.3 \pm 1.4	95.7 \pm 0.3	95.8 \pm 0.1
AIRPORT	92.4 \pm 1.0	92.8 \pm 0.8	98.0 \pm 0.1	98.2 \pm 0.1
CITSEER	71.8 \pm 0.5	72.7 \pm 0.8	96.8 \pm 0.1	96.7 \pm 0.2
PUBMED	81.2 \pm 0.1	82.1 \pm 0.4	96.5 \pm 0.1	96.7 \pm 0.1
CORA	82.3 \pm 0.6	82.5 \pm 0.6	94.9 \pm 0.3	95.0 \pm 0.5

For reader’s convenience, we show the real time with the running environment *Intel(R) Xeon(R) Gold 6132 CPU @ 2.60GHZ* in TABLE IV. As observed, the run-time to calculate the ORC is related to the scale of a given graph that the cost for a simple graph with fewer edges is small, vice versa, and the computation cost is indeed trivial and affordable. Additionally, the ORC needs to be calculated once only before the training process. So the computation complexity of the training and inference phase is the same with HGCN [9]. To apply ORC to super large-scale graph data, we can also utilize approximation methods, e.g., sinkhorn [61], Jaccard proxy [62].

VII. CONCLUSION

Hyperbolic space shows capability for capturing the hierarchical relationship and has been successfully applied to model graphs with tree-like structures. Though a continuous manifold can be employed to approximate a discrete graph, distortions are inevitable as the structure of a real-world network is complex. In this work, we integrate the intrinsic graph structure into the continuous hyperbolic embedding space via the discrete Ricci curvature. As expected, Ricci curvature facilitates the node to perceive the role and the hierarchy it belongs to, helping accelerate the hierarchical formation as well as alleviate the distortion in local clusters or cliques. The superiority of the proposal is demonstrated by extensive experiments. Curvature is a geometric notion with appealing and descriptive properties for both network and continuous space. Via the interaction of curvatures, we can build proper connections for a graph and the embedding space to obtain high-quality representations, which is a promising direction to advance geometric learning.

In the future, we will consider the following curvature, that is, Ricci flow. Ricci flow derived from Ricci curvature is a more interesting geometric concept, which may bring new results for graph embedding and graph machine learning.

REFERENCES

- [1] T. N. Kipf and M. Welling, “Semi-supervised classification with graph convolutional networks,” in *ICLR*, 2017.
- [2] P. Veličković, G. Cucurull, A. Casanova, A. Romero, P. Liò, and Y. Bengio, “Graph attention networks,” in *ICLR*, 2018.
- [3] W. L. Hamilton, R. Ying, and J. Leskovec, “Inductive representation learning on large graphs,” in *NeurIPS*, 2017, pp. 1025–1035.
- [4] K. Xu, W. Hu, J. Leskovec, and S. Jegelka, “How powerful are graph neural networks?” in *ICLR*, 2019.
- [5] M. Nickel and D. Kiela, “Poincaré embeddings for learning hierarchical representations,” in *NeurIPS*, 2017, pp. 6338–6347.
- [6] —, “Learning continuous hierarchies in the lorentz model of hyperbolic geometry,” in *ICML*. PMLR, 2018, pp. 3779–3788.
- [7] O. Ganea, G. Bécigneul, and T. Hofmann, “Hyperbolic neural networks,” in *NeurIPS*, 2018, pp. 5345–5355.

- [8] G. Bouchard, S. Singh, and T. Trouillon, "On approximate reasoning capabilities of low-rank vector spaces," in *AAAI spring symposia*, 2015.
- [9] I. Chami, Z. Ying, C. Ré, and J. Leskovec, "Hyperbolic graph convolutional neural networks," in *NeurIPS*, 2019, pp. 4868–4879.
- [10] Q. Liu, M. Nickel, and D. Kiehl, "Hyperbolic graph neural networks," in *NeurIPS*, 2019, pp. 8230–8241.
- [11] A. Gu, F. Sala, B. Guel, and C. Ré, "Learning mixed-curvature representations in product spaces," in *ICLR*, 2019.
- [12] Y. Ollivier, "Ricci curvature of markov chains on metric spaces," *Journal of Functional Analysis*, vol. 256, no. 3, pp. 810–864, 2009.
- [13] R. Forman, "Bochner's method for cell complexes and combinatorial ricci curvature," *Discrete and Computational Geometry*, vol. 29, no. 3, pp. 323–374, 2003.
- [14] J. Jost and S. Liu, "Ollivier's ricci curvature, local clustering and curvature-dimension inequalities on graphs," *Discrete & Computational Geometry*, vol. 51, no. 2, pp. 300–322, 2014.
- [15] W. Ambrose *et al.*, "A theorem of myers," *Duke Mathematical Journal*, vol. 24, no. 3, pp. 345–348, 1957.
- [16] J. Klicpera, A. Bojchevski, and S. Günnemann, "Predict then propagate: Graph neural networks meet personalized pagerank," *ICLR*, 2019.
- [17] C. Ma, L. Ma, Y. Zhang, J. Sun, X. Liu, and M. Coates, "Memory augmented graph neural networks for sequential recommendation," *arXiv preprint arXiv:1912.11730*, 2019.
- [18] C. Morris, M. Ritzert, M. Fey, W. L. Hamilton, J. E. Lenssen, G. Rattan, and M. Grohe, "Weisfeiler and leman go neural: Higher-order graph neural networks," in *AAAI*, vol. 33, 2019, pp. 4602–4609.
- [19] Y. Zhang, H. Zhu, Z. Song, P. Koniusz, and I. King, "COSTA: Covariance-preserving feature augmentation for graph contrastive learning," in *KDD*, 2022, pp. 2524–2534.
- [20] Y. Zhang, H. Zhu, Z. Meng, P. Koniusz, and I. King, "Graph-adaptive rectified linear unit for graph neural networks," in *WWW*, 2022, pp. 1331–1339.
- [21] M. Yang, Z. Meng, and I. King, "FeatureNorm: L2 feature normalization for dynamic graph embedding," in *ICDM*, 2020, pp. 731–740.
- [22] Z. Song, Y. Zhang, and I. King, "Towards an optimal asymmetric graph structure for robust semi-supervised node classification," in *KDD*, 2022, pp. 1656–1665.
- [23] Z. Song, Z. Meng, Y. Zhang, and I. King, "Semi-supervised multi-label learning for graph-structured data," in *CIKM*. ACM, 2021, pp. 1723–1733.
- [24] V. Khrulkov, L. Mirvakhabova, E. Ustinova, I. Oseledets, and V. Lempit-sky, "Hyperbolic image embeddings," in *CVPR*, 2020, pp. 6418–6428.
- [25] C. Gulcehre, M. Denil, M. Malinowski, A. Razavi, R. Pascanu, K. M. Hermann, P. Battaglia, V. Bapst, D. Raposo, A. Santoro *et al.*, "Hyperbolic attention networks," in *ICLR*, 2019.
- [26] F. Sala, C. De Sa, A. Gu, and C. Re, "Representation tradeoffs for hyperbolic embeddings," in *ICML*, 2018, pp. 4460–4469.
- [27] Y. Chen, M. Yang, Y. Zhang, M. Zhao, Z. Meng, J. Hao, and I. King, "Modeling scale-free graphs for knowledge-aware recommendation," *WSDM*, 2022.
- [28] M. Yang, M. Zhou, J. Liu, D. Lian, and I. King, "HRCF: Enhancing collaborative filtering via hyperbolic geometric regularization," in *WWW*, 2022.
- [29] J. Sun, Z. Cheng, S. Zuberi, F. Pérez, and M. Volkovs, "HGCF: Hyperbolic graph convolution networks for collaborative filtering," in *WWW*, 2021, pp. 593–601.
- [30] H. Wang, D. Lian, H. Tong, Q. Liu, Z. Huang, and E. Chen, "Hypersocrec: Exploiting hyperbolic user and item representations with multiple aspects for social-aware recommendation," *TOIS*, p. 1–28, 2021.
- [31] M. Yang, Z. Li, M. Zhou, J. Liu, and I. King, "HICF: Hyperbolic informative collaborative filtering," in *KDD*, 2022, pp. 2212–2221.
- [32] Y. Zhang, X. Wang, C. Shi, X. Jiang, and Y. F. Ye, "Hyperbolic graph attention network," *TBD*, 2021.
- [33] J. Liu, M. Yang, M. Zhou, S. Feng, and P. Fournier-Viger, "Enhancing hyperbolic graph embeddings via contrastive learning," in *NeurIPS 2nd SSL workshop*, 2022.
- [34] M. Yang, M. Zhou, M. Kalander, Z. Huang, and I. King, "Discrete-time temporal network embedding via implicit hierarchical learning in hyperbolic space," in *KDD*, 2021, pp. 1975–1985.
- [35] A. Lou, I. Katsman, Q. Jiang, S. Belongie, S.-N. Lim, and C. De Sa, "Differentiating through the Fréchet mean," *arXiv preprint arXiv:2003.00335*, 2020.
- [36] Y. Zhang, X. Wang, C. Shi, N. Liu, and G. Song, "Lorentzian graph convolutional networks," in *WWW*, 2021, pp. 1249–1261.
- [37] W. Peng, J. Shi, Z. Xia, and G. Zhao, "Mix dimension in poincaré geometry for 3d skeleton-based action recognition," in *ACM MM*, 2020, pp. 1432–1440.
- [38] S. Wang, X. Wei, C. N. dos Santos, Z. Wang, R. Nallapati, A. Arnold, B. Xiang, S. Y. Philip, and I. F. Cruz, "Mixed-curvature multi-relational graph neural network for knowledge graph completion," pp. 1761–1771, 2021.
- [39] S. Wang, X. Wei, C. N. Nogueira dos Santos, Z. Wang, R. Nallapati, A. Arnold, B. Xiang, P. S. Yu, and I. F. Cruz, "Mixed-curvature multi-relational graph neural network for knowledge graph completion," in *WWW*, 2021, pp. 1761–1771.
- [40] S. Zhu, S. Pan, C. Zhou, J. Wu, Y. Cao, and B. Wang, "Graph geometry interaction learning," in *NeurIPS*, vol. 33, 2020, pp. 7548–7558.
- [41] C.-C. Ni, Y.-Y. Lin, J. Gao, and X. Gu, "Network alignment by discrete ollivier-ricci flow," in *International Symposium on Graph Drawing and Network Visualization*. Springer, 2018, pp. 447–462.
- [42] C.-C. Ni, Y.-Y. Lin, J. Gao, X. D. Gu, and E. Saucan, "Ricci curvature of the internet topology," in *INFOCOM*. IEEE, 2015, pp. 2758–2766.
- [43] E. Jonckheere, M. Lou, F. Bonahon, and Y. Baryshnikov, "Euclidean versus hyperbolic congestion in idealized versus experimental networks," *Internet Mathematics*, vol. 7, no. 1, pp. 1–27, 2011.
- [44] J. Sia, E. Jonckheere, and P. Bogdan, "Ollivier-ricci curvature-based method to community detection in complex networks," *Scientific reports*, vol. 9, no. 1, pp. 1–12, 2019.
- [45] C.-C. Ni, Y.-Y. Lin, F. Luo, and J. Gao, "Community detection on networks with ricci flow," *Scientific reports*, vol. 9, no. 1, pp. 1–12, 2019.
- [46] H. Farooq, Y. Chen, T. T. Georgiou, A. Tannenbaum, and C. Lenglet, "Network curvature as a hallmark of brain structural connectivity," *Nature communications*, vol. 10, no. 1, pp. 1–11, 2019.
- [47] A. K. Simhal, K. L. Carpenter, S. Nadeem, J. Kurtzberg, A. Song, A. Tannenbaum, G. Sapiro, and G. Dawson, "Measuring robustness of brain networks in autism spectrum disorder with ricci curvature," *Scientific reports*, vol. 10, no. 1, pp. 1–8, 2020.
- [48] Z. Ye, K. S. Liu, T. Ma, J. Gao, and C. Chen, "Curvature graph network," in *ICLR*, 2019.
- [49] J. Topping, F. Di Giovanni, B. P. Chamberlain, X. Dong, and M. M. Bronstein, "Understanding over-squashing and bottlenecks on graphs via curvature," *arXiv preprint arXiv:2111.14522*, 2021.
- [50] J. M. Lee, "Smooth manifolds," in *Introduction to Smooth Manifolds*. Springer, 2013, pp. 1–31.
- [51] A. A. Ungar *et al.*, "The hyperbolic square and mobius transformations," *Banach Journal of Mathematical Analysis*, vol. 1, no. 1, pp. 101–116, 2007.
- [52] P. Van der Hoorn, G. Lippner, C. Trugenberger *et al.*, "Ollivier curvature of random geometric graphs converges to ricci curvature of their riemannian manifolds," *arXiv preprint arXiv:2009.04306*, 2020.
- [53] A. G. Ache and M. W. Warren, "Ricci curvature and the manifold learning problem," *Advances in Mathematics*, vol. 342, pp. 14–66, 2019.
- [54] K. Verbeek and S. Suri, "Metric embedding, hyperbolic space, and social networks," in *Proceedings of the thirtieth annual symposium on Computational geometry*, 2014, pp. 501–510.
- [55] K. Huang and M. Zitnik, "Graph meta learning via local subgraphs," *NeurIPS*, vol. 33, 2020.
- [56] W. L. Hamilton, R. Ying, and J. Leskovec, "Inductive representation learning on large graphs," in *NeurIPS*, 2017, pp. 1025–1035.
- [57] F. Wu, A. Souza, T. Zhang, C. Fifty, T. Yu, and K. Weinberger, "Simplifying graph convolutional networks," in *ICML*. PMLR, 2019, pp. 6861–6871.
- [58] G. Bachmann, G. Bécigneul, and O. Ganea, "Constant curvature graph convolutional networks," in *ICML*. PMLR, 2020, pp. 486–496.
- [59] D. Cushing, R. Kangaslampi, V. Lipiäinen, S. Liu, and G. W. Stagg, "The graph curvature calculator and the curvatures of cubic graphs," *Experimental Mathematics*, pp. 1–13, 2019.
- [60] B. Loisel and P. Romon, "Ricci curvature on polyhedral surfaces via optimal transportation," *Axioms*, vol. 3, no. 1, pp. 119–139, 2014.
- [61] M. Cuturi, "Sinkhorn distances: Lightspeed computation of optimal transport," *NeurIPS*, vol. 26, pp. 2292–2300, 2013.
- [62] S. Pal, F. Yu, T. J. Moore, R. Ramanathan, A. Bar-Noy, and A. Swami, "An efficient alternative to ollivier-ricci curvature based on the jaccard metric," *arXiv preprint arXiv:1710.01724*, 2017.